

A New Method for Twisted Wire Crosstalk Estimation Based on GA-BP Neural Network Algorithm

Wu Zhang, Yongji Wu, Jiafei Ding, Yang Zhao, and Mingyuan He

Department of Electrical and Automation Engineering
Nanjing Normal University, Nanjing, 210046, China
m13571872250@163.com, 597692488@qq.com, 2269533002@qq.com, zhaoyang2@njnu.edu.cn,
704256104@qq.com

Abstract – Based on the research of genetic algorithm (GA) to optimize the BP neural network algorithm, this paper proposes a method for predicting twisted wire crosstalk based on the algorithm. Firstly, the equivalent circuit model of a multi-conductor transmission line is established, combined with the method of similarity transformation, the second-order differential transmission line equations are decoupled into n groups of independent two-conductor transmission line equations, and the crosstalk is finally solved. Then the mathematical model of the twisted wire is established and its structural characteristics are analyzed, and the GA-BP neural network algorithm is used to realize the mapping of the electromagnetic parameter matrix of the twisted wire and the position of the twisted wire. Finally, the mapping relationship is substituted into the transmission line equation, and the near-end crosstalk (NEXT) and the far-end crosstalk (FEXT) of an example three-core twisted wire are predicted based on the idea of cascade combined. By comparing with the transmission line matrix method (TLM), it can be seen that the method proposed in this paper is in good agreement with the crosstalk results obtained by the electromagnetic field numerical method, which verifies the effectiveness of the algorithm proposed in this paper.

Index Terms – Back propagation neural network (BPNN) algorithm, crosstalk, genetic algorithm (GA), multi-conductor transmission line (MTL).

I. INTRODUCTION

As the main body of the car circuit network, the car wiring harness connects the various electrical and electronic components of the car and makes them function, but it also provides a carrier for the propagation of interference signals. It can increase the noise level of the adjacent equipment and wires, destroy the data, affect the conducted and radiated emissions of the system, and make the overall electromagnetic compatibility performance of the vehicle drop drastically [1]. Therefore, in

the early stage of automotive EMC performance design, crosstalk is the primary prediction target [2, 3]. However, due to the uncertainty of the parasitic parameters of the twisted wire, there is a lack of research concerning internal crosstalk.

The research method of non-uniform transmission line crosstalk is also applicable to twisted wires; the only difference is the lack of effective methods for extracting parasitic parameters of twisted wires [4, 5]. Based on the cascade concept, the non-uniform transmission line can be equivalent to the cascade of finite micro-element segments, and a single micro-element segment can be approximated as a uniform transmission line, and its transmission line equation can be characterized by its RLCG parasitic parameter matrix [6, 7]. Most of the existing literature uses computational electromagnetic numerical methods to extract the parasitic parameters of non-uniform transmission lines. Literature [8] introduced the FDTD algorithm when analyzing the transmission line system, and then obtained the time domain difference model of the transmission line, and finally extracted the parasitic parameter matrix from the field solution. In [9], the finite element method (FEM) is used to solve the problem of electromagnetic parameter extraction, and the extraction is based on the equivalent dielectric constant to deal with the layered problem of the medium. Literature [10] discusses a simple model for approximating the per-unit-length parameters of a lossy cable providing a smooth transition from low to high frequencies.

Numerical methods have both precision defects and application conditions, but modern artificial intelligence algorithms can better deal with the coexistence of computational efficiency and computational accuracy. Literature [11] is based on this idea and introduces BP neural network to construct the nonlinear mapping relationship between the twisted wire electromagnetic parameter matrix and the axial extension of the twisted wire, and finally combines the finite difference time domain algorithm (FDTD) to complete the crosstalk prediction of the twisted wire. BP neural network has a strong non-linear

mapping ability and can escape the constraint of mathematical formulas [12, 13], to complete the one-to-one correspondence between any position of the twisted wire and its RLCG parasitic parameter matrix. As the sample data stimulate it, the BP neural network adjusts the weight threshold of the hidden layer and the output layer to achieve the approximate output of the network's expected output of the sample data, and self-learning. The essence is to dynamically adjust the connection weight, so that the algorithm may fall into a local extreme value. In addition, the BP neural network relies on the initial network weight threshold. After initialization with different weight thresholds, the network will often acquire solutions with different accuracy [14–16]. To prevent the BP neural network from falling into the local optimum, this paper proposes the GA-optimized BP neural network algorithm model. A genetic algorithm can solve the problem of the BP neural network falling into local optimality. It optimizes the weights and thresholds of BP neural networks and solves the sensitivity problem of BP neural networks to initial weights.

II. MULTI-CONDUCTOR TRANSMISSION LINE MODELING ANALYSIS

A. Multi-conductor transmission line equation

Based on the idea of a cascade, the analysis of multi-conductor transmission lines can be micro-processed, the multi-conductor transmission line is composed of a finite length of micro-element small segments, in which the multi-conductor transmission line can be equivalent to the equivalent circuit form, which is convenient further analyze its crosstalk effect, as shown in Fig. 1. The coupling effect of the transmission line can be fully characterized by this model, with high accuracy. Among them, l_{ii} , l_{jj} represent the self-inductance per unit length of the transmission line, l_{ij} represents the mutual inductance per unit length between the transmission lines. r_{ii} , r_{jj} respectively represent the resistance per unit length of the transmission line. c_{ij} represents the mutual coupling capacitance per unit length between the transmission lines, c_{ii} , c_{jj} represents the coupling capacitance of the transmission lines to the ground. g_{ij} , g_{ii} represent the leakage conductance per unit length between the transmission lines.

Based on the above analysis, the multi-conductor transmission line equation is derived from the perspective of Kirchhoff's law. For the loop between the i -th conductor and the reference conductor, the multi-conductor transmission line equation can be obtained:

$$\begin{cases} \frac{\partial}{\partial z} \mathbf{V}(z,t) = -\mathbf{R}\mathbf{I}(z,t) - \mathbf{L} \frac{\partial}{\partial t} \mathbf{I}(z,t) \\ \frac{\partial}{\partial z} \mathbf{I}(z,t) = -\mathbf{G}\mathbf{V}(z,t) - \mathbf{C} \frac{\partial}{\partial t} \mathbf{V}(z,t) \end{cases} \quad (1)$$

Where RLCG is the parasitic parameter matrix of the transmission line.

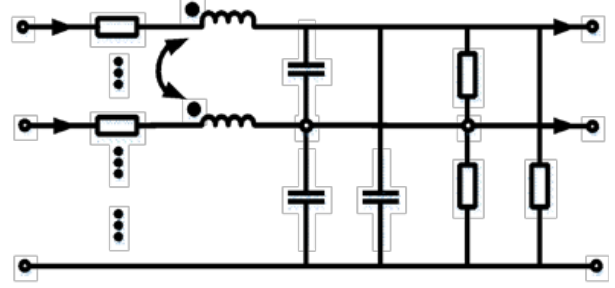


Fig. 1. The equivalent circuit of a multi-conductor transmission line per unit length.

B. Similarity transformation decoupled MTL equations

Equation (1) removes time-domain related t parameters to form a frequency-domain multi-conductor transmission line equation:

$$\begin{cases} d\bar{\mathbf{U}}(z)/dz = -\mathbf{Z}\bar{\mathbf{I}}(z) \\ d\bar{\mathbf{I}}(z)/dz = -\mathbf{Y}\bar{\mathbf{U}}(z) \end{cases} \quad (2)$$

Where \mathbf{Z} is the impedance matrix per unit length, and \mathbf{Y} is the admittance matrix per unit length, which can be expressed by the RLCG parasitic parameters:

$$\begin{cases} \mathbf{Z} = \mathbf{R} + j\omega\mathbf{L} \\ \mathbf{Y} = \mathbf{G} + j\omega\mathbf{C} \end{cases} \quad (3)$$

Differentiating the position z of the transmission line on both sides of the first-order coupling differential equation (2) and substituting them for each other can be converted into a decoupled second-order ordinary differential equation:

$$\begin{cases} d^2\bar{\mathbf{U}}(z)/dz^2 = \mathbf{Z}\mathbf{Y}\bar{\mathbf{U}}(z) \\ d^2\bar{\mathbf{I}}(z)/dz^2 = \mathbf{Y}\mathbf{Z}\bar{\mathbf{I}}(z) \end{cases} \quad (4)$$

The idea of similar transformation method is used to further decoupling [17], removing the coupling between the cable voltage and the current. Through similar transformation, $\mathbf{Z}\mathbf{Y}$ and $\mathbf{Y}\mathbf{Z}$ are diagonalized at the same time, so as to realize the decoupling of the above second-order equation, there are:

$$\begin{cases} \mathbf{T}_U^{-1}\mathbf{Z}\mathbf{Y}\mathbf{T}_U = \boldsymbol{\gamma}^2 \\ \mathbf{T}_I^{-1}\mathbf{Y}\mathbf{Z}\mathbf{T}_I = \boldsymbol{\gamma}^2 \end{cases} \quad (5)$$

Modulus transformation $\Sigma U(z)$ and $\Sigma I(z)$ can obtain the solution of homogeneous differential equations after decoupling:

$$\begin{cases} \bar{\mathbf{U}}_m(z) = \mathbf{U}_m^+ e^{-\boldsymbol{\gamma}z} + \mathbf{U}_m^- e^{\boldsymbol{\gamma}z} \\ \bar{\mathbf{I}}_m(z) = \mathbf{I}_m^+ e^{-\boldsymbol{\gamma}z} - \mathbf{I}_m^- e^{\boldsymbol{\gamma}z} \end{cases} \quad (6)$$

Where $\bar{\mathbf{U}}_m = \mathbf{T}_U^{-1}\mathbf{U}\mathbf{T}_U = \mathbf{T}_I^{-1}\mathbf{I}$.

The crosstalk after modulus transformation can be expressed as:

$$\bar{\mathbf{U}}(z) = \mathbf{Y}^{-1}\mathbf{T}_I\boldsymbol{\gamma}\mathbf{T}_I^{-1}\mathbf{I}_m^+ e^{-\boldsymbol{\gamma}z} + \mathbf{I}_m^- e^{\boldsymbol{\gamma}z}. \quad (7)$$

Combining the port conditions and reducing the undetermined coefficients, the crosstalk can be finally

obtained. It can be seen that, for a multi-conductor transmission line, only the impedance matrix Z and the admittance matrix Y need to be obtained to actually solve the parallel cable crosstalk.

III. GA-BP NEURAL NETWORK ALGORITHM TO EXTRACT PARASITIC PARAMETERS OF TWISTED RLCG

A. Twisted wire structure analysis

From the perspective of the axial direction of the transmission line, the twisted wire can be seen as a combination of countless continuously rotating cross sections. Taking the three-core twisted wire shown in Fig. 2 as an example, the phase difference of the initial point of the single wire is 120° , and the cross-section of the twisted wire at the corresponding axial point can be obtained by continuous rotation of the initial cross-section. When O_1 turns to the O_2 position, O_2 turns to the O_3 position, and O_3 turns to the O_1 position, it means that the rotation angle is 120° . The definition of the pitch p shows that the axial extension distance of the strands is a single pitch at this time.

Figure 3 illustrates the continuous rotation of the cross-section of the three-core twisted wire within a single pitch and the axial extension of the wire. It can be seen from Fig. 3 that the initial cross-section of the three-core twisted wire is rotated through the angle to obtain a cross-section consistent with the initial cross-sectional shape, only the difference in the serial number of the transmission line is artificially defined. In this paper, the position of the axial extension of the three-twisted wire at this time is defined as the transposition of the three-core twisted wire, which defines the axial coordinate of the transposition point as $mp/3, m = 0, 1, 2, \dots$. By analogy, the corresponding axial length of the twisted wire transposition and its corresponding rotation angle can be

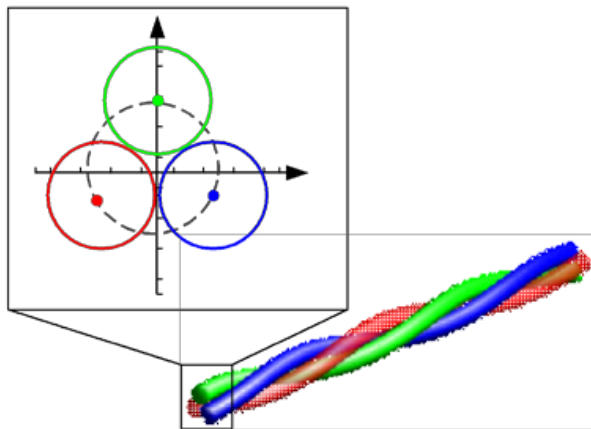


Fig. 2. Three-core twisted wire model.

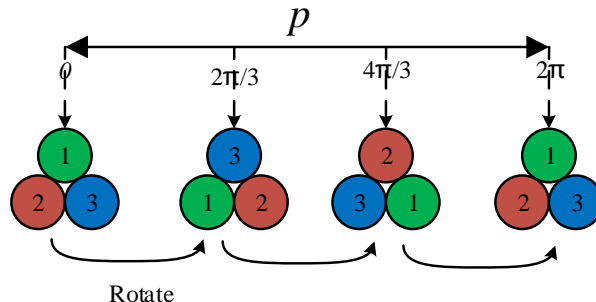


Fig. 3. Three-core twisted single-pitch conversion model.

expressed as:

$$\begin{cases} l = mp/n \\ \theta = 2m\pi/n \end{cases} \quad (8)$$

Where m is a constant and n is the number of cores.

With the axial extension of the twisted wire, the cross-sectional shape of the twisted wire is also changing, which corresponds to the change of the parasitic parameters of the twisted wire, that is, there is a nonlinear mapping relationship between the axial coordinate of the twisted wire and the parasitic parameters of the twisted wire. The functional relationship can be expressed as:

$$f(l) = [\mathbf{R}, \mathbf{L}, \mathbf{C}, \mathbf{G}]. \quad (9)$$

Where $[\mathbf{R}, \mathbf{L}, \mathbf{C}, \mathbf{G}]$ is the parasitic parameter matrix of the twisted wire, and l represents the horizontal distance between any cross-section of the twisted wire and the initial cross-section.

Through the structural analysis of the twisted wire and the relationship between the axial length of the transposition and its corresponding rotation angle, the coordinates of any point on the twisted wire can be converted into the rotation angle of the twisted wire at that point, expressed as:

$$\begin{cases} \theta = \frac{l}{p}2\pi, 0 \leq l \leq p \\ \theta = \frac{(l-mp)}{p}2\pi + 2m\pi, mp \leq l \leq (m+1)p \leq d \end{cases} \quad (10)$$

Where l is the axial coordinate of the strand, θ is the rotation angle, p is the pitch, and d is the total length of the strand.

From formula (10), formula (9) can be transformed into:

$$f(\theta) = [\mathbf{R}, \mathbf{L}, \mathbf{C}, \mathbf{G}]. \quad (11)$$

B. BP neural network

The BP neural network is introduced in [12] to approximate the mapping relationship between the independent variable and the dependent variable with high precision, avoiding the difficulty of mathematical formulas to deal with nonlinear problems.

The neural network takes the rotation angle as input, and the output is RLCG parasitic parameters. Selecting

a single hidden layer can determine the topology of the BP neural network as shown in Fig. 4. Among them, the weight from the input layer to the t -th hidden layer is expressed as $w_{1,t}$, the weight from the t -th hidden layer to the m -th output layer is expressed as $w_{t,m}$. The number of hidden layer neurons t is an empirical range value, affected by the number of input elements n and the number of output elements m can be expressed as:

$$t = (m+n)^{0.5} + a, (a = 1, 2, \dots, 10). \quad (12)$$

The output of the corresponding BP neural network is the RLCG parasitic parameter matrix. However, the matrix cannot exist directly as the output quantity, and the matrix needs to be transformed. Study the problem of twisted wires in the initial pitch, analyze the training data of training the neural network within the line length, and combine the theory of multi-conductor transmission line to know that RLCG is a diagonal matrix. Therefore, the RLCG matrix only needs the upper or lower triangular elements as the research target. The diagonal and upper triangular elements in the $R'L'C'G'$ matrix are extracted.

$$\begin{cases} \mathbf{R}'' = [r_{11}, \dots, r_{1n}, r_{22}, r_{23}, \dots, r_{2n}, \dots, r_{nn}] \\ \mathbf{L}'' = [l_{11}, \dots, l_{1n}, l_{22}, l_{23}, \dots, l_{2n}, \dots, l_{nn}] \\ \mathbf{G}'' = [g_{11}, \dots, g_{1n}, g_{22}, g_{23}, \dots, g_{2n}, \dots, g_{nn}] \\ \mathbf{C}'' = [c_{11}, \dots, c_{1n}, c_{22}, c_{23}, \dots, c_{2n}, \dots, c_{nn}] \end{cases} \quad (13)$$

Reorganize $\mathbf{R}''\mathbf{L}''\mathbf{C}''\mathbf{G}''$ into a vector as:

$$\mathbf{Y} = [\mathbf{R}''\mathbf{L}''\mathbf{C}''\mathbf{G}']^T = [y_1, y_2, \dots, y_m]^T. \quad (14)$$

Where y represents the value of the sample element of the RLCG parameter matrix, where the total number of elements in y is $m=2n(1+n)$ and n is the number of cores. It can be seen that the output of the BP neural network is a column vector organized by diagonal and upper triangular elements of the twisted RLCG parameter matrix, m is the number of outputs, and one element of the corresponding column vector corresponds to one element in the twisted RLCG parameter matrix. The BP neural net-

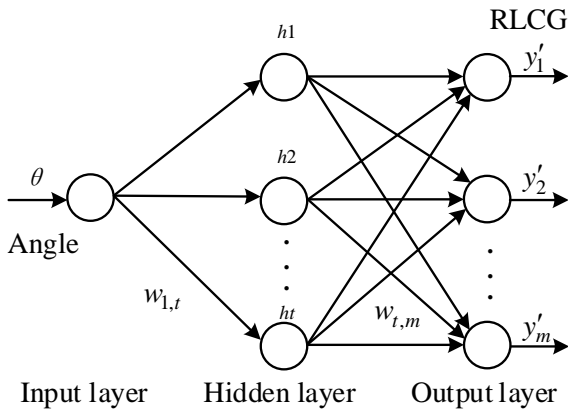


Fig. 4. Topological structure of the multi-core twisted cable neural network.

work prediction model is the twisted wire parasitic parameter extraction model. Through the above analysis, the input of the parasitic parameter extraction network is the axis coordinate of the twisted wire and the output is the column vector of the RLCG parameter matrix.

C. Genetic algorithm optimizes BP neural network

First, the application effect of the BP neural network is greatly affected by its weight and the initial value of the threshold. Therefore, when the neural network is forwarded, it is easy to fall into a local minimum and affect the prediction effect; secondly, the BP neural network uses the gradient descent method, when optimizing complex objective functions, the required training time is too long, which leads to too many iterations of the algorithm and slower convergence. Based on the above two reasons, this study uses the genetic (GA) algorithm [18] to optimize the weights and thresholds of the BP neural network, forming a new GA-BP neural network algorithm, and applying it to the analysis and calculation of the parasitic parameters of the twisted wire.

The genetic algorithm mainly includes three steps (selection, crossover, and mutation), and its modeling process is as follows:

Selection: According to individual fitness, select good individuals to pass on to the next generation. The calculation method used in this study is the roulette method.

$$\begin{cases} f_i = k/F_i \\ p_i = f_i / \sum_{i=1}^N f_i \end{cases} \quad (15)$$

Where f_i is the fitness of individual i ; F_i is the fitness function of individual i ; k is the selection coefficient; p_i is the selection probability of individual i .

Crossover: The GA algorithm uses entity coding in the calculation process. This study uses the real number crossover method.

$$\begin{cases} a_{xi} = a_{xi}(1-b) + a_{yi}b \\ a_{yi} = a_{yi}(1-b) + a_{xi}b \end{cases} \quad (16)$$

Where a_{xi} is the i position of the x th chromosome, a_{yi} is the i position of the y th chromosome, and b is a random number, $0 \leq b \leq 1$.

Mutation: After selecting an individual, convert certain genes into other genes with a certain probability.

$$a_{ij} = \begin{cases} a_{ij} + (a_{ij} - a_{\max}) * f(g), r > 0.5 \\ a_{ij} + (a_{\min} - a_{ij}) * f(g), r \leq 0.5 \end{cases} \quad (17)$$

$$f(g) = r_2 \left(1 - \frac{g}{G_{\max}} \right)^2 \quad (18)$$

Where a_{\max} is the upper bound of gene a_{ij} , a_{\min} is the lower bound of gene a_{ij} , r_2 is a random number, g is the number of iterations, G_{\max} is the maximum number of iterations, r is a random number, $0 \leq r \leq 1$.

The steps for GA to optimize BP are as follows:

- (1) The training samples are normalized. Use maximum and minimum normalization to compress the training samples to speed up the training speed while preserving the characteristics of the data.
- (2) Initialize the BP neural network algorithm. Determine the topology of the BP neural network, determine the number of hidden layer units, learning rate and activation function and other network parameters based on the training samples, and generate the corresponding network topology.
- (3) Initialize the genetic algorithm. Generate the initial population, randomly generate the initial values of the weights and thresholds, and use them as individuals in the population to perform real number coding. Define the chromosome code length l , then for the BP neural network of 1- M - N topology:

$$l = 1 * M + M * N + M + N. \quad (19)$$

- (4) Determine the fitness function. The root mean square error MSE of the test data is used as the fitness evaluation function to evaluate the chromosomes.

$$\text{fitness} = \text{MSE} = \frac{1}{N} \sum_{i=1}^N (t_{sim}(i) - y_i)^2. \quad (20)$$

Where N is the number of samples in the training set; $t_{sim}(i)$ is the predicted value of the i th sample; y_i is the actual value of the i th sample. Therefore, the minimum fitness function value when the algorithm iteration stops is the optimal solution.

- (5) Choose the parent. Sort the individuals according to their fitness, and use the roulette algorithm to screen out 2 individuals as parents. Calculate the best-fitness of the individual, and record the chromosome code of the best individual.
- (6) Random crossover. The parent uses the weight and threshold of each layer of the network as genes and uses a random crossover algorithm to combine genes with a certain crossover probability p_1 to generate new offspring.
- (7) Mutation operation. In the generation of offspring, there is a certain probability that some individuals in p_2 will mutate, and the weights and thresholds of the mutated individuals will be re-assigned to generate new genes.
- (8) Iteratively update to solve the optimal individual. If the fitness of the best individual of the next generation is better than that of the previous generation, update the best fitness and the best individual; otherwise, keep the same and eliminate the worst individual.
- (9) Iteration stop condition. When the stop condition is not met, select some individuals with high fitness

from the original population and the newly generated offspring to form a new population, and repeat steps (5) to (8) to continue solving the weights and thresholds of the satisfied conditions. When the stopping condition is satisfied, that is, the maximum number of iterations or the accuracy condition is satisfied, the chromosome encoding information in bestchrom is the optimal weight and threshold, and the optimal solution is generated.

IV. VERIFICATION AND ANALYSIS

A. Comparison between BPNN and GA-BPNN

This article takes three-core twisted wire as an example to verify and analyze the method proposed. Strand parameters are shown in Table 1. The specific distribution graph on the ground is shown in Fig. 5.

Taking the cross-section of the wire harness with a rotation degree of 0° in Fig. 5. as the reference cross-section, the RLCG parameter matrix within a single pitch is extracted using Ansys Q3D simulation software. At high frequencies, the resistance per unit length of the conductor increases with the square root of the frequency due to the skin effect [19], and the conductance of the homogeneous medium surrounding the conductor is also frequency dependent. The RLCG parameter in the model in this article uses the value extracted at 500 MHz

In summary, the neural network takes the upper triangular element of the RLCG parameter as the output

Table 1: Three-core twisted cable

Parameters	Values
Single wire radius	0.6 mm
Single wire conductivity	58000000 S/m
Single wire insulation thickness	0.6 mm
Insulation layer relative permittivity	2.7
Pitch	1000 mm
Height	3.5 mm

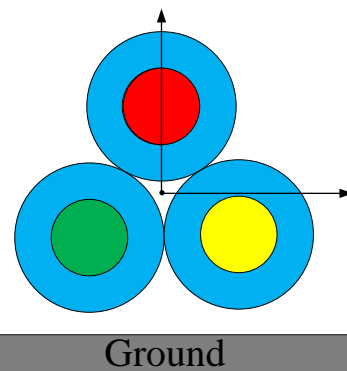


Fig. 5. Reference cross-section of three-core twisted wire model.

and the cross-section rotation angle θ as the output. According to the hidden layer neuron empirical formula (12), the value range of hidden layer neurons is [5–15]. The MSE value under the number of neurons in each hidden layer is compared in turn, and the optimal t value is selected, that is, the hidden layer. The number of layered neurons is 12. Therefore, for the three-core twisted wire, set the BP neural network topology to 1-12-24, and the chromosome code length is 336. At the same time, the error accuracy is set to $1e-6$, the learning rate is 0.05, the population size is 50, the number of iterations is 100, the crossover probability p_1 is 0.4, and the mutation probability p_2 is 0.2.

Bring the corresponding angles of the last ten sets of samples into the parameter prediction model to obtain the corresponding prediction output value. The relative error results before and after the algorithm optimization are shown in Fig. 6. The average relative errors of BPNN

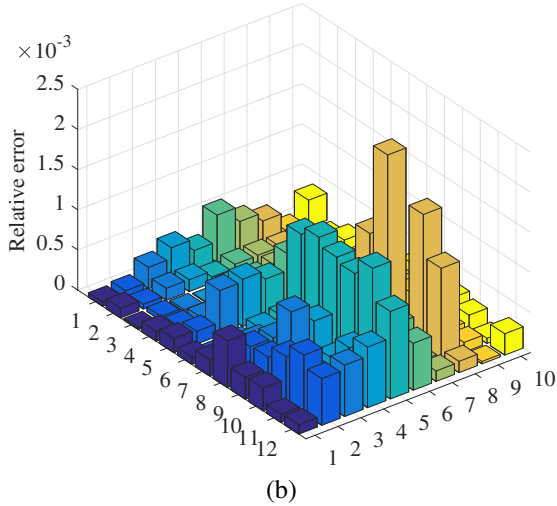
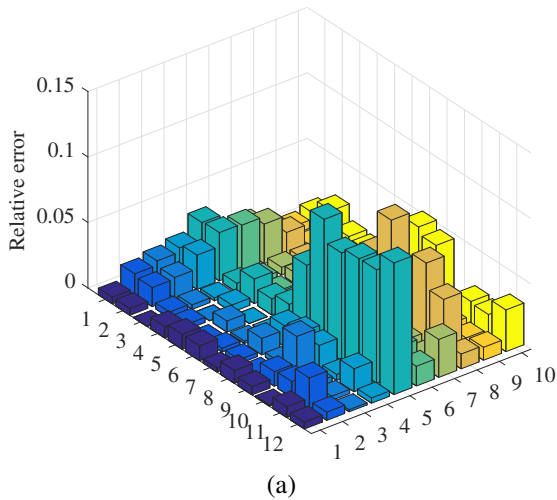


Fig. 6. Neural network relative error: (a) BP-NN and (b) GA-BPNN.

and GA-BPNN are 1.66% and 0.03%, respectively, and the GA algorithm significantly improves the prediction accuracy of the neural network.

B. Comparison between BPNN and GA-BPNN

The transmission line matrix method (TLM) is the core algorithm of the electromagnetic simulation software CST Cable Studio. A three-core twisted wire circuit model is established in CST shown in Fig. 7. For the three-core twisted wire, any wire is used as the excitation wire, which is defined as line 1. The other two lines are used as disturbed lines, which are defined as line 2 and line 3, respectively.

The crosstalk obtained by using two methods in 0.1MHz-1GHz are shown in Fig. 8. Due to the symmetry of the twisted wire structure, at the initial frequency of 0.1MHz, the NEXT performance of this simulation on lines 2 and 3 is -61.17dB , and the GA-BPNN algorithm performance is -61.47dB ; GA-BPNN algorithm and simulation tend to be consistent, and fluctuate around -18dB at high frequencies after a steady increase. At the initial frequency of 0.1MHz, the FEXT performance of the simulation on lines 2 and 3 is -66.32dB , and the GA-BPNN algorithm performance is -66.73dB ; the GA-BPNN algorithm and simulation tend to be consistent and fluctuate around -14dB at high frequencies after a steady increase.

The average values of the crosstalk values obtained by the proposed algorithm and simulation in different frequency bands are shown in Tables 2 and 3. The results show that the algorithm proposed in this paper is consistent with the simulation results.

Through the analysis of the crosstalk results, it can be seen that the NEXT and FEXT solved by the proposed algorithm are basically the same as the CST simulation values. In general, the crosstalk based on the proposed algorithm shows good consistency with the simulation experiment results in the crosstalk variation trend, and also shows good accuracy in the numerical value.

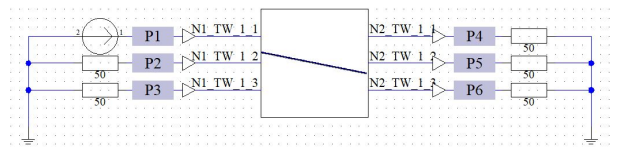


Fig. 7. CST simulation model.

Table 2: The average value of NEXT in different frequency bands of Line 2 (dB)

Frequency/MHz	0.1~100	100~500	500~1000
GA-BP	-19.28	-19.66	-19.92
Simulation	-19.02	-19.27	-17.53

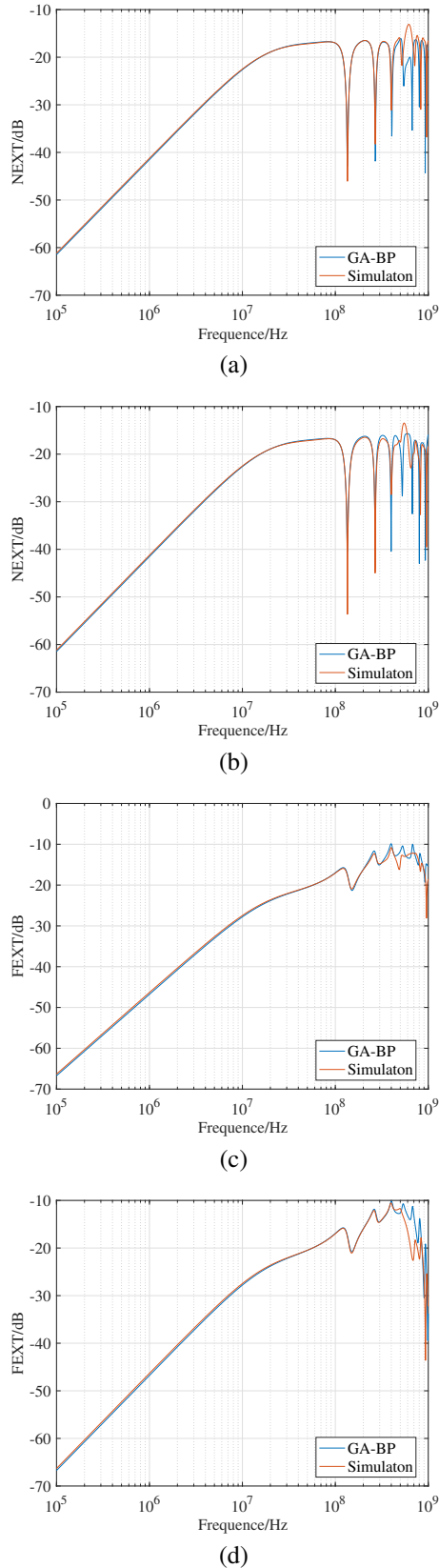


Fig. 8. (a) line 2 NEXT, (b) line 3 NEXT, (c) line 2 FEXT, and (d) line 3 FEXT.

Table 3: The average value of FEXT in different frequency bands of Line 2 (dB)

Frequency/MHz	0.1~100	100~500	500~1000
GA-BP	-22.52	-14.13	-13.61
Simulation	-22.16	-14.80	-14.76

V. CONCLUSION

This paper proposes a method for extracting the RLCG parameter matrix of twisted wires based on the GA-BP algorithm. In fact, any spatial wiring that satisfies a certain mathematical relationship can extract a high-precision RLCG parameter matrix through this method. In this paper, a multi-conductor transmission line crosstalk model is established, and the second-order differential transmission line equations are decoupled into n groups of independent two-conductor transmission line equations by the method of similarity transformation, and the crosstalk is finally solved. The effectiveness and applicability of the method in this paper to predict the twisted wire crosstalk are verified by numerical experiments. In engineering applications, the results of NEXT and FEXT predictions can directly provide theoretical reference for the layout, type selection, and parameter adjustment of the line.

ACKNOWLEDGMENT

The manuscript is funded by the National Institute of Technology National Natural Science Foundation of China, approval number: 52107005.

REFERENCES

- [1] M. O'Hara and J. Colebrooke, "Automotive EMC test harnesses: standard lengths and their effect on conducted emissions," *IEEE International Symposium on Electromagnetic Compatibility*, vol. 1, pp. 233-236, May 2003.
- [2] K. Armstrong, "EMC for the functional safety of automobiles why EMC testing is insufficient, and what is necessary," *IEEE International Symposium on Electromagnetic Compatibility*, pp. 1-6, Oct. 2008.
- [3] S. Frei, R. G. Jobava, and D. Topchishvili, "Complex approaches for the calculation of EMC problems of large systems," *International Symposium on Electromagnetic Compatibility*, vol. 3, pp. 826-831, Aug. 2004.
- [4] A. Shoory, M. Rubinstein, and A. Rubinstein, "Simulated NEXT and FEXT in twisted wire pair bundles," *10th International Symposium on Electromagnetic Compatibility*, York, UK, pp. 266-271, Sep. 2011.
- [5] P. Manfredi, Daniël De Zutter, and D. V. Ginste, "Analysis of non-uniform transmission lines with an iterative and adaptive perturbation technique,"

- IEEE Transactions on Electromagnetic Compatibility*, vol. 58, no. 3, pp. 859-867, Jun. 2016.
- [6] M. Tang and J. Mao, "A precise time-step integration method for transient analysis of lossy non-uniform transmission lines," *IEEE Transactions on Electromagnetic Compatibility*, vol. 50, no. 1, pp. 166-174, Feb. 2018.
- [7] C. Jullien, P. Besnier, M. Dunand, and I. Junqua, "Advanced modeling of crosstalk between an unshielded twisted pair cable and an unshielded wire above a ground plane," *IEEE Transactions on Electromagnetic Compatibility*, vol. 55, no. 1, pp. 183-194, Feb. 2013.
- [8] K. Afrooz and A. Abdipour, "Efficient method for time-domain analysis of lossy nonuniform multi-conductor transmission line driven by a modulated signal using FDTD technique," *IEEE Transactions on Electromagnetic Compatibility*, vol. 54, no. 2, pp. 482-494, Apr. 2012.
- [9] R.-S. Chen, E. K.-N. Yung, C. H. Chan, D. X. Wang, and D. G. Fang, "Application of the SSOR preconditioned CG algorithm to the vector FEM for 3D full-wave analysis of electromagnetic-field boundary-value problems," *IEEE Transactions on Microwave Theory & Techniques*, vol. 50, no. 4, pp. 1165-1172, Aug. 2002.
- [10] F. M. Tesche, "A simple model for the line parameters of a lossy coaxial cable filled with a nondispersive dielectric," *IEEE Transactions on Electromagnetic Compatibility*, vol. 49, no. 1, pp. 12-17, Feb. 2007.
- [11] C. Yang, W. Yan, Y. Zhao, Y. Chen, C. Zhu, and Z. Zhu, "Analysis on RLCG parameter matrix extraction for multi-core twisted cable based on back propagation neural network algorithm," *IEEE Access*, vol. 2, no. 1, pp. 16-19, Aug. 2019.
- [12] T. Liu, H. Mei, Q. Sun, and H. Zhou, "Application of neural network in fault location of optical transport network," *China Communications*, vol. 16, no. 10, pp. 214-225, Oct. 2019.
- [13] W. Wu, G. Feng, Z. Li, and Y. Xu, "Deterministic convergence of an online gradient method for BP neural networks," *IEEE Transactions on Neural Networks*, vol. 16, no. 3, pp. 533-540, May 2005.
- [14] A. Yang, Y. Zhuansun, C. Liu, J. Li, and C. Zhang, "Design of intrusion detection system for internet of things based on improved BP neural network," *IEEE Access*, vol. 7, pp. 106043-106052, Jul. 2019.
- [15] G. Chen, L. Li, Z. Zhang, and S. Li, "Short-term wind speed forecasting with principle-subordinate predictor based on Conv-LSTM and Improved BPNN," *IEEE Access*, vol. 8, no. 3, pp. 67955-67973, Mar. 2020.
- [16] W. Wang, Q. Zhu, Z. Wang, X. Zhao, and Y. Yang, "Research on indoor positioning algorithm based on SAGA-BP neural network," *IEEE Sensors Journal*, vol. 22, no. 4, pp. 3736-3744, Feb. 2022.
- [17] C. R. Paul, "Decoupling the multiconductor transmission line equations," *IEEE Transactions on Microwave Theory and Techniques*, vol. 44, no. 8, pp. 1429-1440, Aug. 1996.
- [18] G. Oliveri and A. Massa, "Genetic algorithm (GA)-enhanced almost difference set (ADS)-based approach for array thinning," *Microwaves Antennas and Propagation Letters*, vol. 5, no. 3, pp. 305-315, Mar. 2015.
- [19] N. Idir, Y. Weens, and J. Franchaud, "Skin effect and dielectric loss models of power cables," *IEEE Transactions on Dielectrics and Electrical Insulation*, vol. 16, no. 1, pp. 147-154, Feb. 2009.



Wu Zhang was born in Anhui Province, China. He received his B.S degree from the School of Electrical Engineering and Automation from Xi'an University of Technology, Xi'an, China, in 2020. He is currently working toward a master's degree in electrical engineering at Nanjing Normal University, Nanjing, China. His main research interests include multi-conductor transmission lines and EMC.



Yongji Wu was born in Shanxi Province, China. He received a bachelor's degree from Shanxi Institute of Engineering and Technology in 2018 and is currently studying for a master's degree in electrical engineering at Nanjing Normal University. The main research direction

is the electromagnetic compatibility of the secondary equipment of the substation and the power system.



Yang Zhao received his B.E., M.E., and Ph.D. degree all in power electronic technology from Nanjing University of Aeronautics and Astronautics, Nanjing, China, in 1989 and 1992, and 1995, respectively. He is currently the professor with Nanjing Normal University. His research inter-

ests are in the areas of Electromagnetic Compatibility, Power Electronics and Automotive Electronics.



Jiafei Ding was born in Nantong City, Jiangsu Province in 1996. He graduated from Nanjing Normal University with a bachelor's degree in 2019 and is currently studying for a master's degree at the School of Electrical and Automation Engineering of Nanjing Normal University.

His main research interests are signal integrity and electromagnetic compatibility of power systems.



Mingyuan He was born in Gansu Province, China. He graduated from Hohai University in 2017 with a bachelor's degree. Currently studying for a master's degree in electrical engineering at Nanjing Normal University. The main research direc-

tions are new energy station control, power system optimization operation and stability control.